RSC Advances

PAPER

View Article Online
View Journal | View Issue

Cite this: *RSC Adv.*, 2020, **10**, 40171

Synthesis of Ag_2S colloidal solutions in D_2O heavy water

Stanislav I. Sadovnikov * and Aleksandr I. Gusev

Received 14th September 2020
Accepted 28th October 2020

DOI: 10.1039/d0ra07853k

rsc.li/rsc-advances

For the first time, colloidal solutions of silver sulfide are synthesized by chemical deposition from solutions of silver nitrate and sodium sulfide in heavy water D_2O. In the synthesis, sodium citrate was used as a stabilizer. The sizes of Ag_2S quantum dots in colloidal solutions were estimated by dynamic light scattering and transmission electron microscopy. The size of silver sulfide quantum dots in colloidal solutions in heavy water that were prepared from reaction mixtures with different concentrations of reagents is from 3 to 19–20 nm. An increase in the concentration of silver nitrate and a decrease in the concentration of sodium citrate in the initial reaction mixtures lead to a small increase in the size of Ag_2S quantum dots in the synthesized colloidal solutions. Colloidal silver sulfide solutions synthesized using D_2O heavy water retain the stability and constant size of the nanoparticles after storage for more than 100 days. The calculated exciton diameter for Ag_2S is about 3 nm, and is consistent with experimental observations.

1. Introduction

Ag_2S QDs can be used in infrared detectors,[1–3] in resistance-switches and nonvolatile memory devices.[4–6] Ag_2S QDs can be used in the manufacture of nanocomposite photocatalysts and materials for conversion of solar energy into electrical energy.[7,8] Stable Ag_2S QDs possess high fluorescence emission from the UV to NIR region.

Nanostructured silver sulfide including quantum dots has been produced by different methods such as hydrochemical deposition, template method, sol–gel method, synthesis in microemulsions, as well as by sonochemical, hydrothermal, solvothermal, electrochemical, microwave and other techniques. Detailed description of various methods for the synthesis of nanostructured silver sulfide is given in review.[9] However, many of these methods are not universal and allow synthesis of nanostructured silver sulfide only in one form: either nanopowders, or films, or heteronanostructures. Bad control of the size and non-uniform broad size distribution of nanoparticles, use of multistage (3–4 stages) sequential processes, complicated technique and special defenders, the raised temperatures, rare and expensive reagents are the main disadvantages of many preparation methods of nanostructured Ag_2S.

Different synthetic methods of Ag_2S QDs have been summarized in review.[10] Recently a group of Prof. J. G. Tang, using a reverse microemulsion approach, synthesized uniform 3–8 nm Ag_2S nanoparticles.[11,12]

The chemical deposition from aqueous solutions is the most simple and widespread method used for the synthesis of nanocrystalline sulfide powders and colloidal solutions of sulfide quantum dots including Ag_2S QDs.

Usually colloidal solutions of silver sulfide synthesize by hydrochemical deposition from aqueous solutions of silver nitrate $AgNO_3$ and sodium sulfide Na_2S. Solution of trisodium citrate dihydrate (sodium citrate) $Na_3C_6H_5O_7 \cdot 2H_2O \equiv Na_3Cit$ uses as an electrostatic stabilizer, disodium salt of ethylenediaminetetraacetic acid (Trilon B) is used as the complexing agent. Chemical deposition with using sodium citrate Na_3Cit is a well-known, simple and reliable universal green method which allows preparing colloidal solutions of Ag_2S QDs.

Not only homogeneous size distribution, but also the exact control of the real form (sphere, ellipsoid *etc.*) of Ag_2S QDs is required for their application in electronic and optoelectronic devices.

Modern diagnostics of nanosystems uses various types of radiation to obtain information about the structure of nano-objects in volume and on surfaces. The special properties of low-energy neutrons with a wavelength of about 0.15 nm (1.5 Å), which include thermal and cold neutrons, make it possible to effectively use their scattering in studies of solids, liquids, and colloidal systems. Neutron diffraction methods, in particular small-angle neutron scattering (SANS),[13–15] are sensitive to structural organization features at a level of 1–100 nm.

Small angle scattering of X-rays (SAXS) and neutrons (SANS) is one of the most effective methods for studying structures with sizes from one to several hundred nanometers. The diffraction pattern is the result of interference of rays scattered elastically and coherently on the sample, that is, without changing the

Institute of Solid State Chemistry, Ural Branch of the Russian Academy of Sciences, Ekaterinburg 620990, Russia. E-mail: sadovnikov@ihim.uran.ru

wavelength and phase. The main advantage of small-angle scattering is the possibility of using it to study disordered objects and in the absence of the need for special sample preparation. The basic formulas that relate the scattering intensity to the structure of an object are determined only by the scattering power of the inhomogeneities and the contrast of their electron density with respect to the main matrix.[13,14,16] Thus, small-angle scattering allows one to study objects of various physical nature and state of aggregation, including nanoparticles in an amorphous matrix (glass) or colloidal particles (quantum dots) in solution.[17,18] Small-angle neutron scattering is generally applicable for studying the structure, shape (ball, ellipsoid, prism, cylinder, *etc.*), the ratio of the length and width of nanoparticles smaller than 100 nm in size.

When studying colloidal solutions by the small-angle neutron scattering, it should be taken into account that the irradiating neutrons from the reactor practically does not scattered on the nucleus of a hydrogen atom, but is absorbed by the hydrogen. Therefore, when using ordinary water as a solvent, the diffraction pattern is practically impossible to obtain. In addition to the proton, a neutron is present in the nucleus of a deuterium atom; therefore, neutrons from a reactor are scattered elastically on the deuterium nucleus. For this reason, to study the structure of colloidal solutions by small angle neutron scattering, heavy water D_2O should be used as a solvent instead of ordinary H_2O water. Indeed, coherent scattering amplitudes of hydrogen and deuterium atoms differ in magnitude and sign. This leads to the fact that the densities of coherent scattering amplitudes of light and heavy water also differ in magnitude and sign (-0.56×10^{10} cm^{-2} and $+6.39 \times 10^{10}$ cm^{-2}, respectively).[19,20]

In small-angle neutron scattering, contrast variation plays an important role in studying the fine structure of nano-objects. The use of heavy water or a mixture of light and heavy water changes the scattering contrast between particles and solvent and allows us to study the heterogeneity of nano-objects.[19,21] Measurements in heavy water can significantly reduce the concentration of the studied colloidal solutions compared to the concentration of colloidal solutions obtained using ordinary (light) water. Small-angle neutron scattering covers the wavelength range from 0.1 to 2.0 nm (1–20 Å), which corresponds to scattering vectors from 1 to 10^{-6} $Å^{-1}$.[19] Such a wide range of scattering vectors allows the study of colloidal solutions with a very low concentration of nanoparticles.

To study colloidal solutions using small angle neutron scattering, it is most effective to use colloidal solutions obtained using heavy water.

It is known that the solvent has a significant effect on the rate of chemical reactions, which is associated, in particular, with the dielectric constant of the solvent. The dielectric constant of ordinary H_2O water and heavy D_2O water at room temperature is ~81.0 and 78.2, respectively. Reactions involving D_2O usually proceed at a slower rate than with H_2O, and the solubility of salts in heavy water is slightly less (5–10%) than in ordinary H_2O.[22] Recently, the difference between the standard reduction potentials of H_2O and D_2O during hydrothermal synthesis of iron-containing solids has been established.[23] However, the effect of heavy water on the dissolution of salts has been studied very poorly, and the formation of sulfide colloidal solutions in heavy water has not been studied at all.

Nobody has obtained colloidal solutions of silver sulfide in heavy water, suitable for studying by small-angle neutron scattering. An essential property of these colloidal solutions should be their stability. In the literature there is no information about such colloidal solutions. From private reports it is known that attempts to synthesize stable colloidal solutions of silver sulfide in heavy water were failed. For example, stable colloidal solutions of Ag_2S in ordinary water can be synthesized in solutions of silver nitrate $AgNO_3$, sodium sulfide Na_2S using 3-mercaptopropyl-trimethoxysilane (MPS) $HSC_3H_6Si(OCH_3)_3$ ($C_6H_{16}O_3SSi$) as a stabilizer.[24] However, with the same synthesis in D_2O heavy water using MPS, colloidal silver sulfide solutions are unstable: Ag_2S nanoparticles precipitate 3–4 days after the synthesis of solutions.

Present work is devoted to study of the synthesis of stable colloidal solutions of silver sulfide in D_2O heavy water as a solvent. Such research is carried out for the first time in the world. The main characteristics of Ag_2S quantum dots synthesized in colloidal solutions of silver sulfide in heavy water are determined. Potentially synthesized colloidal solutions are intended for the subsequent study of the real fine structure of Ag_2S quantum dots using small-angle neutron scattering. The study of fine structure is not available for other methods. Direct measurements of synthesized colloidal solutions by small-angle neutron scattering will be the subject of independent research.

2. Experimental

For the synthesis of colloidal solutions of Ag_2S based on D_2O, the same procedure was used as for the synthesis of colloidal solutions based on H_2O described in study.[25] Colloidal solutions of Ag_2S were synthesized by chemical deposition from aqueous solutions of silver nitrate $AgNO_3$, sodium sulfide Na_2S and sodium citrate $Na_3C_6H_5O_7 \equiv Na_3Cit$ in high-purity deionized heavy water D_2O. The D_2O content in the used heavy water was not less than 99.9 mol%, the admixture of light water H_2O was less than 0.1 mol%. The electrical conductivity of heavy water did not exceed 5 $\mu S\ cm^{-1} = 0.0005\ S\ m^{-1}$.

A transparent stable colloidal solution with a solid dispersed phase of Ag_2S (nano-Ag_2S) was obtained by chemical deposition in D_2O heavy water. Solutions of sodium sulfide Na_2S and silver nitrate $Ag(NO_3)_2$ in heavy water with the same concentrations of 50 mmol L^{-1} were used as initial solutions. It was shown earlier[22] that reaction mixtures with such concentrations are supersaturated by silver and sulfur ions; therefore, the synthesis of Ag_2S was carried out for a very short time.

The synthesis was carried out at a temperature of 298 K in the dark. Sodium citrate in the synthesis of Ag_2S in heavy water D_2O plays the role of a stabilizing agent to prevent nanoparticle growth. The stabilizing role of sodium citrate in the hydrochemical synthesis of nanostructured silver sulfide in ordinary (light) water was described earlier in study.[9,25–28] In colloidal solutions of Ag_2S QDs in heavy water, citrate ions are attached on the surface of the Ag_2S nanoparticles and form a negatively charged citrate layer, which prevents sulfide nanoparticles from coming together.

In aqueous solutions with low S^{2-} ion concentration, sodium citrate can reduce Ag^{+} ions to form silver metal nanoparticles[9,26–28] and form a citrate shell on Ag_2S particles.[9,29–33] Therefore, to obtain colloidal solutions of silver sulfide without Ag impurities and without a citrate shell, reaction mixtures with a small relative excess of sodium sulfide Na_2S and a minimum concentration of Na_3Cit were used. The synthesis was carried out in the dark in a neutral medium at pH ≈ 7 by the following reaction scheme

$$2AgNO_3 + (1+\delta)Na_2S \xrightarrow{Na_3C_6H_5O_7} Ag_2S\downarrow + 2NaNO_3, \quad (1)$$

where $0.01 \geq \delta \geq 0.5$ is a small excess of Na_2S, needed for synthesizing Ag_2S colloidal solutions without admixture of Ag.

For the synthesis, solutions of $AgNO_3$, Na_2S, and Na_3Cit previously prepared in heavy water D_2O were used. The synthesis was performed in the following order: to 5 mL of a silver nitrate solution was poured in 5 mL of a sodium citrate (stabilizer) solution, and the resulting solution was mixed with 10 mL of a Na_2S solution for 1–2 seconds.

The stable colloidal solutions with Ag_2S quantum dots with an average size less than 20 nm were prepared from reaction mixtures 1–8 with silver nitrate concentrations C_{AgNO_3} from 0.3125 to 2.5 mmol L^{-1} (Table 1). Earlier, reaction mixtures of the same compositions were used for the synthesis of Ag_2S colloidal solutions in ordinary H_2O water.[25] The identical reaction mixtures were used to compare the sizes of Ag_2S nanoparticles synthesized in aqueous colloidal solutions on heavy D_2O and ordinary H_2O water.

The size (hydrodynamic diameter D_{DLS}) of Ag_2S quantum dots and the zeta potential ζ were determined directly in the colloidal solutions by non-invasive Dynamic Light Scattering (DLS) method on a Zetasizer Nano ZS facility (Malvern Instruments Ltd.) at a temperature of 298 K. The He–Ne laser with radiation wavelength 633 nm was used as a radiation source, and the detection angle of backscattered light was 173°. To provide the reproducibility of results, the scattering of light and the size of particles was measured in each solution no less than three times. The conductivity of synthesized colloidal solutions was also determined on a Zetasizer Nano ZS instrument.

The synthesized colloidal solutions were dried by sublimation methods in an Alpha 1–2 LD plus freeze dryer (Martin Christ) at an ice condenser temperature of −55 °C (218 K). Dried powders of nanostructured silver sulfide stored in a Vacuum Desiccator Sanplatec MB, evacuated to a residual pressure of 13.3 Pa (0.1 mm Hg).

Dried silver sulfide powders were examined by X-ray diffraction (XRD) method on a Shimadzu XRD-7000 diffractometer in Cu $K\alpha_{1,2}$ radiation. X-ray measurements were performed in the angle interval $2\theta = 20–95°$ with a step of $\Delta(2\theta) = 0.02°$ and scanning time 20 s in each point. The determination of the crystal lattice parameters and final refinement of the structure of the synthesized sulfide powders were carried out with the use of the X'Pert Plus software suite.[34]

The JEOL JEM-2010 transmission electron microscope with 0.14 nm (1.4 Å) lattice resolution was also used to determine the size of Ag_2S quantum dots. The elemental chemical composition of Ag_2S quantum dots was studied on the same microscope with the use of an Phoenix (EDAX) Energy Dispersive Spectrometer with a Si(Li) detector having energy resolution of 130 eV. Colloidal solutions of Ag_2S quantum dots were placed on a copper grid for examination. A copper grid with an aperture diameter of 50 μm was used for TEM observing of nanoparticles. Additionally, one or two layers of hydrocarbon-glue were applied to copper grid.

In addition, the average particle size D (to be more precise, the average size of coherent scattering regions (CSR)) in synthesized dried silver sulfide nanopowders was estimated by XRD method from the diffraction reflection broadening using the dependence of reduced reflection broadening $\beta^*(2\theta) = [\beta(2\theta)\cos\theta]/\lambda$ on the scattering vector $s = (2\sin\theta)/\lambda$.[35]

UV-vis absorption spectra of colloidal solutions of Ag_2S QDs were recorded on a Shimadzu UV-2401 PC spectrophotometer at room temperature.

The photoluminescence (PL) emission spectra of quantum dots were measured under an excitation of 658 nm on a spectrometer FLS920 (Edinburgh Instrument).

3. Discussion

The XRD pattern of silver sulfide nanopowder obtained by sublimation drying of colloidal solution 6 in heavy water D_2O (Table 1) is shown in Fig. 1a. The diffraction reflections of the

Table 1 Composition of reaction mixtures and average size D of silver sulfide quantum dots in colloidal solutions

	Reagent concentration in the reaction mixtures (mmol L^{-1})			D (nm), (synthesis in D_2O)			D (nm),[25] (synthesis in H_2O)	
No.	$AgNO_3$	Na_2S	Na_3Cit	$D_{DLS} \pm 0.5^a$	$D_{DLS} \pm 0.5^b$	D_{TEM}	$D_{DLS} \pm 0.5^a$	D_{TEM}
1	0.3125	0.165	5	3.1	3.5	2–3	2.3	2–3
2	0.3125	0.168	2.5	4.2	5.1	3–5	2.7	2–3
3	0.3125	0.170	1	6.5	7.9	6–7	3.1	2–4
4	0.625	0.313	5	8.7	10.1	8–9	4.2	3–4
5	0.625	0.325	3.75	10.1	10.7	8–10	5.6	5–6
6	2.5	1.30	1	11.7	14.2	10–12	8.0	8–10
7	0.625	0.330	2.5	15.7	17.3	15–16	9.2	8–10
8	0.625	0.335	1.25	18.7	20.0	18–20	10.0	9–11

[a] Quantum dot size corresponding to the maximum of D_{DLS} size distribution. [b] The average quantum dot size according to DLS data.

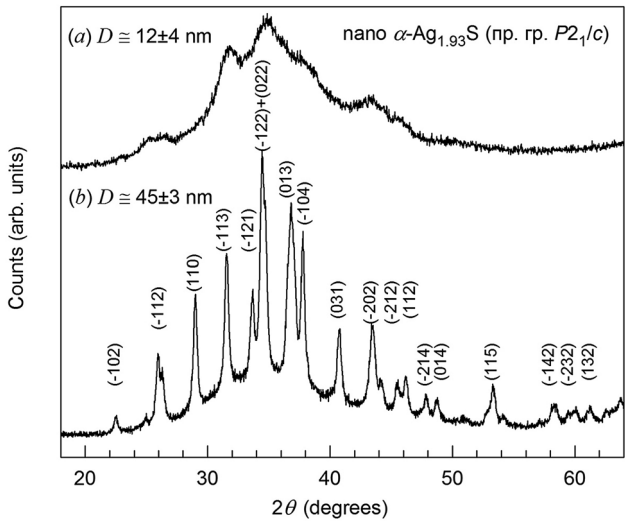

Fig. 1 XRD pattern (a) of nanocrystalline silver sulfide with a monoclinic (space group $P2_1/c$) structure of α-Ag_2S acanthite obtained from colloidal solution 6 in D_2O heavy water (Table 1). For comparison, an XRD pattern[33] (b) of a larger nanopowder of monoclinic silver sulfide with a particle size of ~40–45 nm is shown.

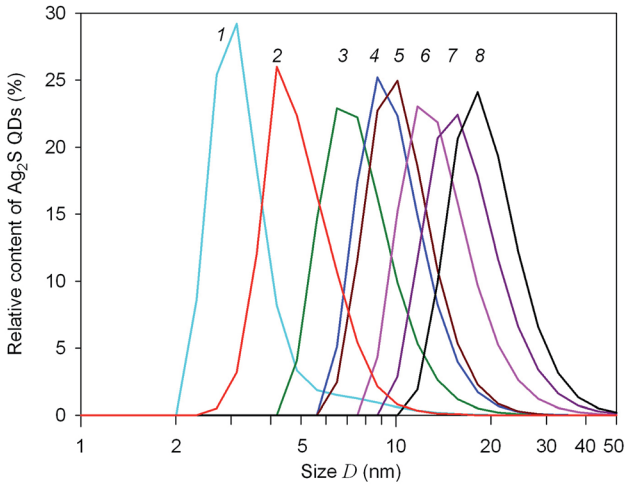

Fig. 2 Size distributions of silver sulfide QDS in colloidal solutions 1–8, measured by the DLS method. The numbering of DLS curves corresponds to the colloidal solutions 1–8 in Table 1. Size D is presented in logarithmic coordinates.

nanopowder are strongly broadened and therefore the reflections located close to each other overlap. For comparison, the XRD pattern[36] of larger Ag_2S nanopowder with particle size ~45 nm deposited from reaction mixture of $AgNO_3$, Na_2S and Na_3Cit with concentrations 50.0, 25.4 and 25.0 mmol L^{-1}, respectively, is shown in Fig. 1b. A quantitative refinement of the structure of the nanopowder obtained from colloidal solution 6 was carried out using the X'Pert HighScore Plus software package.[34] Structure refinement and its comparison with the data of studies[36,37] has shown that the observed set of diffraction reflections corresponds to monoclinic (space group $P2_1/c$) silver sulfide with α-Ag_2S acanthite-type structure. The composition of this nanopowder corresponds to non-stoichiometric silver sulfide $Ag_{1.93\pm0.02}S_{1.00\pm0.01}$. The average size D of CSR estimated from the broadening of non-overlapping diffraction reflections is 12 ± 4 nm. The size of Ag_2S QDs according to DLS and TEM is about 12 nm.

The size distributions of Ag_2S quantum dots in synthesized colloidal solutions, measured by the DLS method, are shown in Fig. 2.

According to DLS data, the average size of Ag_2S quantum dots in colloidal solutions no. 1–8 does not exceed 20 nm (Fig. 2). The quantum dot size corresponding to the maxima of the size distributions D_{DLS} is from 2 to 10 nm (Table 1), and the average quantum dot size D_{aver} in the obtained colloidal solutions varies from ~3 to ~11 nm. With an increase in the concentration of silver nitrate in the initial reaction mixtures, the size of Ag_2S quantum dots in the synthesized colloidal solutions increases slightly. A decrease in the concentration of sodium citrate, all other things being equal, leads to a decrease in the stabilizing effect of Na_3Cit and is also accompanied by some increase in the size of Ag_2S quantum dots (Table 1).

The size of Ag_2S quantum dots in colloidal solutions synthesized in D_2O heavy water is slightly larger than in colloidal solutions in ordinary H_2O water (see Table 1). This may be the result of a slightly lower solubility of sodium citrate in heavy water compared to ordinary water[21] and, as a result, a slight weakening of the stabilizing effect of sodium citrate. However, the qualitative effect of reagent concentrations on the size of silver sulfide quantum dots in colloidal solutions synthesized using heavy water is the same as in colloidal solutions in ordinary H_2O water.[25]

It is known that the zeta potential ζ of quantum dots or nanoparticles in a solution is an indicator of the system stability.[38,39] The absolute values ±(35 ± 15) mV of zeta potential are indicative of electrostatic stability of colloidal solutions. The particles with highly negative or positive surface electric charge are considered as stable particles. The DLS measurements revealed that three days after synthesis of solutions 1–8 their zeta potential ζ was −28 to −18 mV, and the quantum dot size was equal to 3–19 nm. The zeta potential ζ and the size of Ag_2S quantum dots measured 100 days after synthesis of colloidal solutions remained almost unchanged. Small variation of the zeta potential during long-term storage of colloidal solutions and a large negative value of the zeta potential of solutions 1–8 confirm their stability. The conductivity of the synthesized colloidal solutions ranged from 0.067 to 0.108 S m^{-1}. An increase in the conductivity of colloidal solutions in comparison with the heavy D_2O water used confirms the presence of quantum dots with electric charges in solutions. Thus, silver sulfide colloidal solutions synthesized using D_2O heavy water retained the stability and unchanged QDs size after storage for more than 100 days, *i.e.*, they have the same high stability as colloidal solutions synthesized in ordinary water.

Transmission electron microscopy (TEM) confirmed the small size of the Ag_2S quantum dots in the synthesized colloidal solutions.

A TEM image of quantum dots contained in a colloidal solution obtained from reaction mixture 3 with a minimum concentration of sodium citrate is shown in Fig. 3. The size of

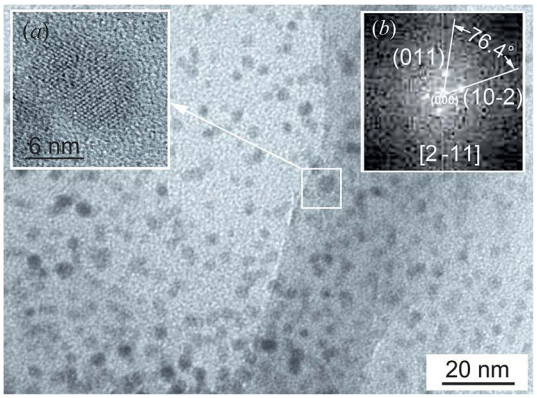

Fig. 3 TEM image of colloidal solution 3 (Table 1). (a) HRTEM image of a quantum dot about 6 nm in size; (b) the selected area of electron diffraction calculated by fast Fourier transform of HRTEM image of this quantum dot.

most quantum dots is from 6 to 7 nm. This is consistent with measurements of the size distribution of Ag_2S quantum dots in this solution by dynamic light scattering (see Fig. 2). As an example, HRTEM image of a quantum dot about 6 nm in size is shown in Fig. 3a. The selected area of electron diffraction (Fig. 3b) was calculated using the Fast Fourier Transform (FFT)[40] of HRTEM image of this quantum dot. A detailed description of the Fast Fourier Transform using the Gatan Microscopy Suite program[37] is given on the site.[41] The observed electron diffraction spots (011) and (1−02) correspond to the [21−1] plane of the reciprocal lattice of monoclinic (space group $P2_1/c$) silver sulfide with α-Ag_2S acanthite structure. To reliably identify the observed diffraction reflections and their indices, it is necessary to calculate the angle φ_{refl} between the reflections with the expected indices $(h_ik_il_i)$ on the selected area of electron diffraction, *i.e.*, the angle between the lines passing through each reflection and the central spot (000). The coincidence of the estimated and experimental φ_{refl} angles unequivocally proves that the indices $(h_ik_il_i)$ are determined correctly.

According to study,[42] the formula for determining the φ_{refl} angle between the reflections $(h_1k_1l_1)_{mon}$ and $(h_2k_2l_2)_{mon}$ in the reciprocal lattice of the monoclinic structure has the form

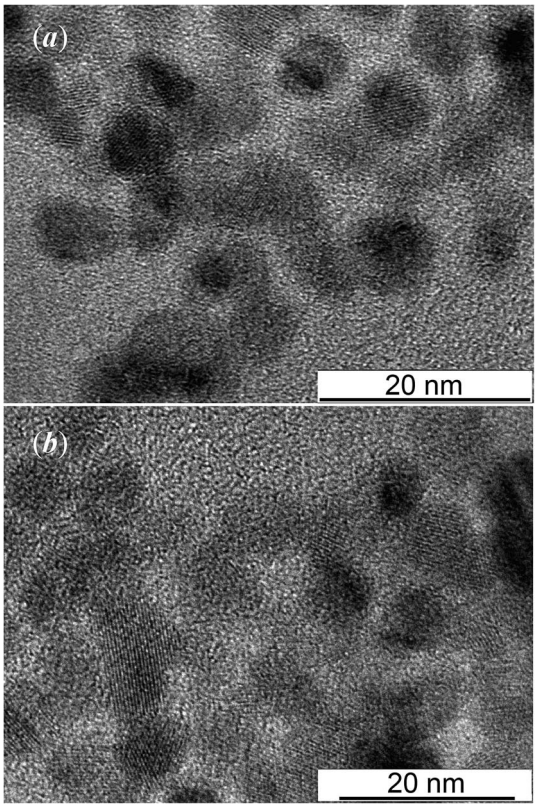

Fig. 4 TEM images (a) and (b) of colloidal solutions 4 and 5, respectively. The numbering corresponds to the Table 1.

Analysis of the HRTEM image (Fig. 3) confirmed that, as a result of synthesis in colloidal solutions in heavy water, monoclinic (space group $P2_1/c$) silver sulfide with α-Ag_2S acanthite structure is actually formed.

Fig. 4 show TEM images of colloidal solutions 4 and 5. It is seen that the size of silver sulfide quantum dots in colloidal solution 4 is from 8 to 9 nm (Fig. 4a). According to TEM, the size of silver sulfide quantum dots in colloidal solution 8–10 nm (Fig. 4b).

Larger silver sulfide quantum dots are observed in colloidal solution 6: the Ag_2S quantum dot from this solution has a size

$$\cos\phi = \frac{h_1h_2/a^2 + k_1k_2/b^2 + [l_1l_2a^2 - (h_1l_2 + h_2l_1)ac\ \cos\beta + h_1h_2c^2\ \cos^2\beta]\Big/(ac\ \sin\beta)^2}{d_1 \times d_2}, \quad (2)$$

where $d_i = \sqrt{(h_i/a)^2 + (k_i/b)^2 + [(l_ia - h_ic\ \cos\beta)/(ac\ \sin\beta)]^2}$ with $i = 1$ or 2.

In Fig. 3b, the angle between the supposed reflections (011) and (−102) is ∼76°. The calculated angle between reflections with such indices for monoclinic silver sulfide should be 76.4° and coincides with the observed angle. Consequently, the reflection indices are defined correctly. The analysis has shown that these reflections are observed along the [2−11] zone axis.

of ∼12 nm (Fig. 5). Fig. 5 clearly shows the interplanar distance 0.187 nm, which coincides with the distance between the atomic planes (014) of silver sulfide with monoclinic (space group $P2_1/c$) structure of the α-Ag_2S acanthite type.[37,43,44] The inset shows the EDX spectrum of Ag_2S nanoparticles from colloidal solution 6.

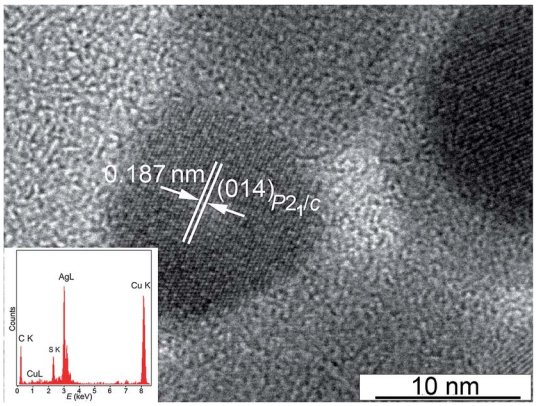

Fig. 5 HRTEM image of a silver sulfide quantum dot from colloidal solution 6 (Table 1). The inset shows the EDX spectrum of Ag_2S nanoparticles.

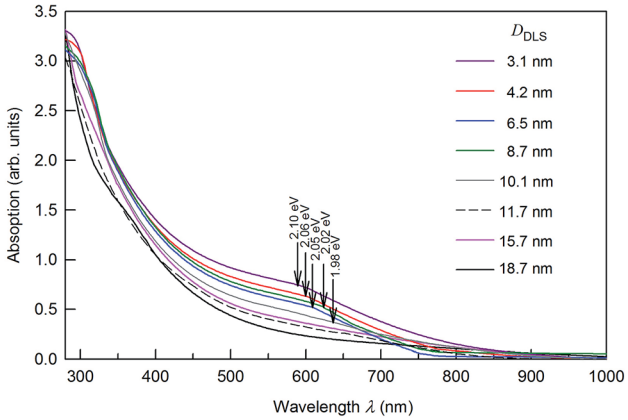

Fig. 6 The UV-vis absorption spectra of colloidal solutions of Ag_2S QDs 60 days after synthesis. The weak absorption peak observed in the spectra of solutions with a quantum dots of size 3.1, 4.2, 6.5, and 8.7 nm at wavelength λ about 280–310 nm corresponds to Ag_2S QDs. The positions of ground state exciton absorption are marked by arrows.

TEM images of colloidal solutions, as well as the sizes of quantum dots according to TEM which given in Table 1, confirm the results of DLS measurements of quantum dot size.

In the EDX spectra obtained using a JEOL JEM-2100 transmission electron microscope, in addition to silver and sulfur, Kα lines of copper Cu from the copper grid are observed, on which the quantum dots under study and a weak Kα line of carbon C from the glue were applied (see Fig. 5, inset). A source of carbon C in colloidal solutions of silver sulfide is also an admixture of the initial reagent – sodium citrate Na_3Cit. The sodium citrate solution is adsorbed on the surface of Ag_2S quantum dots. According to EDX data, impurity oxygen is also present in silver sulfide quantum dots, which is distributed over the surface of the particles, which is reflected in the presence of a weak Kα line of oxygen at 0.525 keV.

According to the EDX results (Fig. 5, inset), minus the impurity elements, the silver and sulfur contents in the synthesized silver sulfide are 83.4 ± 0.5 and 12.8 ± 0.2 wt%, which corresponds to silver sulfide $Ag_{1.96\pm0.02}S_{1.00\pm0.01}$.

The UV-vis absorption spectra of colloidal solutions 1–8 are displayed in Fig. 6. According to the DLS data, the size of Ag_2S QDs in these solutions changes from to 3.1 to 18.7 nm. The UV-vis absorption spectra of the investigated colloidal solutions reveal wide bands (Fig. 6) characteristic of semiconductor QDs in the region from 280 to 800 nm (4.40–1.55 eV) associated with the ground state exciton absorption.

The weak absorption peak observed at ~280–310 nm corresponds to Ag_2S nanoparticles.[45,46] This weak absorption peak is absent in the absorption spectra of Ag_2S QDs with a size more than 8.7 nm. Considering a large experimental data array,[47–49] the absorption spectra of colloidal Ag_2S QDs do not contain a peak corresponding to the ground state exciton absorption. It can be assumed that the considerable contribution to the absorption band of colloidal QDs is associated with the nonstoichiometry of silver sulfide,[36] which is always accompanied by impurity absorption and leads to the absence of features in the absorption spectrum.

The position of the ground state exciton absorption band in the UV-vis absorption spectra of colloidal solutions 1–5 was found from the minimum of the second derivative for the optical absorption spectra with respect to the photon energy. These positions are marked by arrows in Fig. 6.

Fig. 7 presents the size-dependent photoluminescence (PL) emission spectra of Ag_2S colloidal solutions 1–5 in which the fluorescence of Ag_2S quantum dots is tunable from ~1090 to ~1182 nm by increasing the nanoparticle size D_{DLS} from 3.1 to 10.1 nm. PL emission spectra of colloidal solutions 5, 6, 7, and 8 with Ag_2S quantum dots larger 8 nm practically coincide; therefore, only the spectrum of colloidal solution 5 is shown in Fig. 7.

According to,[50] the PL peak for Ag_2S quantum dot with a size about 1.5 nm is observed at a wavelength of ~640 nm (see Fig. 7); the PL emission spectrum of Ag_2S QD with a size about 1.5 nm was measured under an excitation of 785 nm. Perhaps,

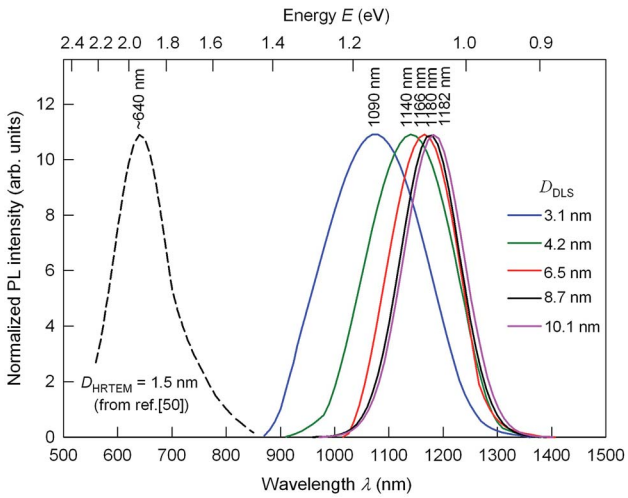

Fig. 7 The size-dependent PL emission spectra of Ag_2S colloidal solutions 1–5 with quantum dots of size D_{DLS} from 3.1 to 10.1 nm under an excitation of 658 nm. For comparison, dashed line show the position of PL emission peak for Ag_2S quantum dots with a size ~1.5 nm.[50] The wavelengths corresponding to the maxima of the PL peaks are indicated.

there was a misprint in study[50] because generally the PL emission wavelength of the sample is longer than it's the excitation wavelength. In study[50] water-soluble Ag_2S quantum dots have been synthesized at heating of mixed solution of mercaptopropionic acid, ethylene glycol, and silver nitrate $AgNO_3$. The PL emission peaks shift from ~1090 to ~1182 nm with the size of Ag_2S quantum dots increasing from ~3.1 to 10.1 nm and keep constant at 1182–1190 nm with increase of the quantum dot size from ~10.1 to 16 nm and further. The continuous blue shift of the PL emission of Ag_2S quantum dots from ~1182 to ~640 nm may be attributed to the strengthened quantum confinement effect and increasing the band gap E_g which resulted from the decreasing Ag_2S quantum dots size (band gap of bulk monoclinic Ag_2S crystals is about 1.0 eV).[25,51] Almost constant position of the PL emission peaks at ~1140–1180 nm for the Ag_2S quantum dots with a boundary value of size 4.2 nm and larger is evidence for transition from the strong quantum confinement regime to the weak quantum confinement regime. The absence of quantum confinement for semiconductor Ag_2S nanocrystals larger 4 nm is in good agreement with the data.[51–53] Thus, we experimentally estimated Ag_2S exciton radius R_{ex} as less than half of boundary value of size 4.2 nm, *i.e.* ≤2.1 nm.

According to,[54] the characteristic size of the Wannier–Mott exciton (or the Bohr radius of the of the first exciton state) in the macroscopic semiconductor is determined by the equation

$$R_{ex} = \frac{\hbar^2 \varepsilon}{e^2}\left(\frac{1}{m_e} + \frac{1}{m_h}\right) = \frac{\hbar^2 \varepsilon}{\mu_{ex} e^2}, \quad (3)$$

where $h = 1.055 \times 10^{-27}$ cm^2 g s^{-1} is the reduced Planck constant, $e = 4.803 \times 10^{-10}$ cm$^{3/2}$ g$^{1/2}$ s^{-1} is the charge on the electron, $\mu_{ex} = m_e m_h/(m_e + m_h)$ is the reduced exciton mass, and m_e and m_h are the electron and hole effective masses. For Ag_2S, dielectric constant ε is about 6, $m_e = 0.286m_0$ and $m_h = 1.096m_0$ ($m_0 = 9.1095 \times 10^{-28}$ g is the free electron mass),[55] respectively. Taking this into account, the reduced exciton mass μ_{ex} for acanthite α-Ag_2S is equal ~$0.23m_0$. At such values of ε, m_e and m_h, the Ag_2S exciton radius R_{ex} which is calculated by the formula (3) is equal to ~1.4 ± 0.1 nm, and the exciton diameter is about 2.8 nm. However in study[55] there are no data on the Brillouin zones estimation or measurement of effective masses by cyclotron resonance. Other effective masses of carriers are given in study:[51] $m_e = 0.42m_0$ and $m_h = 0.81m_0$. These effective masses of electron and hole have been calculated for the lowest conduction band and the highest valence band centered at Γ point of the Brillouin zone of Ag_2S, respectively. Apparently, results of study[51] on the electron and hole effective masses are more correct. According to,[56] real part of dielectric constant ε of silver sulfide is equal to 8.36. For these values m_e, m_h and ε exciton mass μ_{ex} is ~$0.28m_0$, exciton radius R_{ex} is equal to ~1.6 ± 0.1 nm, and the exciton diameter is ~3.2 nm.

Found exciton diameter ~3 ± 0.2 nm of silver sulfide is in satisfactory agreement with experimentally estimated Ag_2S exciton diameter ~4.2 nm which follows from the size-dependent PL emission spectra (see Fig. 7).

Photoluminescence bands of Ag_2S colloidal solutions 1–5 (Fig. 7) are distinguished by the significant Stokes shift of luminescence peaks relative to the position of ground state exciton absorption (see Fig. 6), which increases slightly with decreasing the QD size. The Stokes shift values lie at 0.93–0.99 eV. Fig. 8 shows the change in energies corresponding to the luminescence peaks of colloidal solutions 1–8, depending on the size (diameter) of the Ag_2S QDs. It is clearly illustrated that there is no obvious blue shift of either excitonic energy until the size of QDs is below ~5 nm. As the QD size $D \rightarrow \infty$ increases, the deviation of the excitonic ground state energy from the band gap value of bulk Ag_2S allows one to estimate the exciton binding energy. According to the estimate, it is about 0.05 eV. This is quite close to the exciton binding energy value found in study[51] and equal to 0.096 eV.

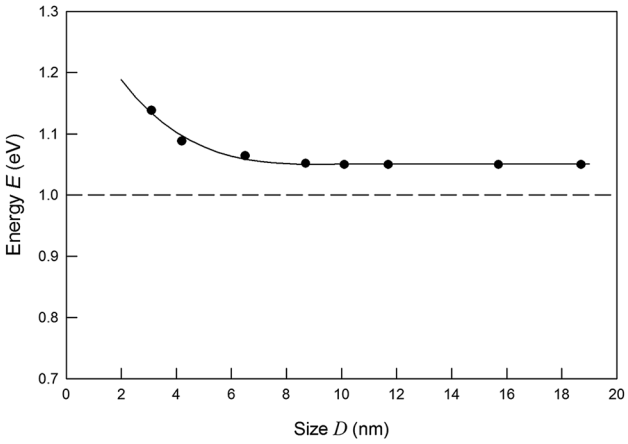

Fig. 8 Exciton energy change with the decreasing of Ag_2S QDs size. Black points are the experimental PL energies, corresponding Fig. 7. Band gap of bulk Ag_2S is shown by dashed line.

4. Conclusion

For the first time, colloidal solutions of silver sulfide quantum dots were synthesized in heavy water D_2O. The synthesized colloidal solutions retain stability and small size of the quantum dots during long-term storage for more than 100 days. The high stability of colloidal solutions synthesized in heavy water is confirmed also by the large negative value of their zeta potential.

Sodium citrate in the synthesis of Ag_2S in heavy water D_2O plays the role of a stabilizing agent. In colloidal solutions of Ag_2S QDs in heavy water, citrate ions are attached on the surface of the Ag_2S QDs and form a negatively charged citrate layer, which prevents sulfide quantum dots from coming together.

The study of colloidal solutions of silver sulfide synthesized in D_2O heavy water by dynamic light scattering, transmission electron microscopy, and X-ray energy dispersive analysis has shown that under these synthesis conditions it was possible to obtain colloidal solutions with silver sulfide QDs from 3 to 19 nm in size with monoclinic (space group $P2_1/c$) α-Ag_2S acanthite structure. Changing the concentration of reagents in the reaction mixtures allows us to control the size of silver sulfide QDs in the resulting colloidal solutions in the range from 2–3 to 20 nm.

An increase in the concentration of silver nitrate and a decrease in the concentration of sodium citrate in the initial reaction mixtures lead to a small increase in the size of Ag_2S QDs in the synthesized colloidal solutions no. 1–5. The size of Ag_2S quantum dots in colloidal solutions synthesized in D_2O heavy water is slightly (by 1–2 nm) larger than in colloidal solutions in ordinary H_2O water. This is evidence of the specific of synthesis and stabilization of colloidal particles of silver sulfide in heavy water compared to ordinary water. It can be assumed that the difference in the size of the quantum dots is associated with different properties of the dispersed medium (heavy and ordinary water), in particular, with a lower solubility of sodium citrate in heavy water compared to ordinary water that leads to a slight weakening of the stabilizing effect of sodium citrate.

The prepared colloidal solutions are suitable for studying the structure of silver sulfide quantum dots by the method of small-angle neutron scattering.

Author contributions

Stanislav I. Sadovnikov: ideas and formulation of research aims, methodology, synthesis and investigations, validation, writing – review and editing, supervision. Aleksandr I. Gusev: analysis of the data, writing – original draft, project administration.

Conflicts of interest

The authors declare that they have no known competing financial interests or personal relationships that could have appeared to influence the work reported in this paper.

Acknowledgements

The authors thank Dr Y. Kuznetsova for her help in the DLS measurement. This study was supported by the Russian Science Foundation (grant no. 19-73-20012) through the Institute of Solid State Chemistry of the Ural Branch of the RAS.

Notes and references

1 T.-Y. Hsu, H. Buhay and N. P. Murarka, Characteristics and applications of Ag_2S films in the millimeter wavelength region, in *Millimeter Optics. SPIE Proc.*, ed. G. A. Tanton, 1980, vol. 259, pp. 38–45.

2 D. Karashanova, D. Nihtianova, K. Starbova and N. Starbov, Crystalline structure and phase composition of epitaxially grown Ag_2S thin films, *Solid State Ionics*, 2004, **171**, 269–275.

3 L. Liu, S. Hu, Y.-P. Dou, T. Liu, J. Lin and Y. Wang, Nonlinear optical properties of near-infrared region Ag_2S quantum dots pumped by nanosecond laser pulses, *Beilstein J. Nanotechnol.*, 2015, **6**, 1781–1787.

4 C. H. Liang, K. Terabe, T. Hasegawa and M. Aono, Resistance switching of an individual Ag_2S/Ag nanowire heterostructure, *Nanotechnology*, 2007, **18**, 485202.

5 Z. Xu, Y. Bando, W. Wang, X. Bai and D. Golberg, Real-time *in situ* HRTEM-resolved resistance switching of Ag_2S nanoscale ionic conductor, *ACS Nano*, 2010, **4**, 2515–2522.

6 A. N. Belov, O. V. Pyatilova and M. I. Vorobiev, Synthesis of Ag/Ag_2S nanoclusters resistive switches for memory cells, *Adv. Nanopart.*, 2014, **3**, 1–4.

7 M. M. El-Nahass, A. A. M. Farag, E. M. Ibrahim and S. Abd-El-Rahman, Structural, optical and electrical properties of thermally evaporated Ag_2S thin films, *Vacuum*, 2004, **72**, 453–460.

8 U. M. Jadhav, S. N. Patel and R. S. Patil, Synthesis of silver sulphide nanoparticles by modified chemical route for solar cell applications, *Res. J. Chem. Sci.*, 2013, **3**, 69–74.

9 S. I. Sadovnikov and A. I. Gusev, Recent progress in nanostructured silver sulfide Ag_2S: from synthesis and nonstoichiometry to properties, *J. Mater. Chem. A*, 2017, **5**, 17676–17704.

10 J. Xue, J. Liu, S. Mao, Y. Wang, W. Shen, W. Wang, L. Huang, H. Li and J. G. Tang, Recent progress in synthetic methods and applications in solar cells of Ag_2S quantum dots, *Mater. Res. Bull.*, 2018, **106**, 113–123.

11 J. Xue, J. X. Liu, Y. M. Liu, H. Li, Y. Wang, D. Sun, W. Wang, L. Huang and J. G. Tang, Recent advances in synthetic methods and applications of Ag_2S-based heterostructure photocatalysts, *J. Mater. Chem. C*, 2019, **7**, 3988–4003.

12 J. Xue, H. Li, J. X. Liu, Y. Wang, Y. M. Liu, D. Sun, W. Wang, L. Huang and J. G. Tang, Facile synthesis of silver sulfide quantum dots by one pot reverse microemulsion under ambient temperature, *Mater. Lett.*, 2019, **242**, 143–146.

13 L. A. Feigin and D. I. Svergun, *Structure analysis by small-angle X-ray and neutron scattering*, Springer, Berlin, 1987, p. 335.

14 D. S. Sivia, *Elementary scattering theory: for X-ray and neutron users*, Oxford University Press, Oxford, 2011, p. 201.

15 O. Glatter and O. Kratky, *Small angle X-ray scattering*, Academic Press, London, 1982, p. 515.

16 J. Ilavsky and P. R. Jemian, Irena: tool suite for modeling and analysis of small-angle scattering, *J. Appl. Crystallogr.*, 2009, **42**, 347–353.

17 Y. V. Kuznetsova, A. A. Rempel, M. Meyer, V. Pipich, S. Gerth and A. Magerl, Small angle X-ray and neutron scattering on cadmium sulfide nanoparticles in silicate glass, *J. Cryst. Growth*, 2016, **447**, 13–17.

18 Y. V. Kuznetsova and A. A. Rempel, Size, zeta potential, and semiconductor properties of hybrid CdS–ZnS nanoparticles in a stable aqueous colloidal solution, *Russ. J. Phys. Chem. A*, 2017, **91**, 1105–1108.

19 Y. Z. Nozik, R. P. Ozerov and K. Hennig, *Structural Neutron Diffraction*, Atomizdat, Moscow, 1979, p. 344.

20 A. M. Balagurov, *Neutron diffraction for solving structural and material science problems*, Moscow State Univer., Moscow, 2017, p. 305.

21 Schmiedel, P. Jörchel, M. Kiselev and G. Klose, Determination of structural parameters and hydration of unilamellar POPC/C12E4 vesicles at high water excess from neutron scattering curves using a novel method of evaluation, *J. Phys. Chem. B*, 2001, **105**, 111–117.

22 A. A. Sunier and J. Baumbach, The solubility of potassium chloride in ordinary and heavy water, *J. Chem. Eng. Data*, 1976, **21**, 335–336.
23 X. Zhou, L. Wang, X. Fan, B. Wilfong, S. z.-C. Liou, Y. Wang, H. Zheng, Z. Feng, C. Wang and E. E. Rodriguez, Isotope effect between H_2O and D_2O in hydrothermal synthesis, *Chem. Mater.*, 2020, **32**, 769–775.
24 Y. V. Kuznetsova, S. V. Rempel, I. D. Popov, E. Y. Gerasimov and A. A. Rempel, Stabilization of Ag_2S nanoparticles in aqueous solution by MPS, *Colloids Surf., A*, 2017, **520**, 369–377.
25 S. I. Sadovnikov, Liquid-phase synthesis of silver sulfide nanoparticles in supersaturated aqueous solutions, *Russ. J. Inorg. Chem.*, 2019, **64**, 1309–1316.
26 R. Chen, N. T. Nuhfer, L. Moussa, H. R. Morris and P. M. Whitmore, Silver sulfide nanoparticle assembly obtained by reacting an assembled silver nanoparticle template with hydrogen sulfide gas, *Nanotechnology*, 2008, **19**, 455604.
27 S. Xiong, B. Xi, K. Zhang, Y. Chen, J. Jiang, J. Hu and H. C. Zeng, Ag nanoprisms with Ag_2S attachment, *Sci. Rep.*, 2013, **3**, 2177.
28 W. Zhang, L. Zhang, Z. Hui, X. Zhang and Y. Qian, Synthesis of nanocrystalline Ag_2S in aqueous solution, *Solid State Ionics*, 2000, **130**, 111–114.
29 P. C. Lee and D. Meisel, Adsorption and surface-enhanced Raman of dyes on silver and gold sols, *J. Phys. Chem.*, 1982, **86**, 3391–3395.
30 A. Tang, Y. Wang, H. Ye, C. Zhou, C. Yang, X. Li, H. Peng, F. Zhang, Y. Hou and F. Teng, Controllable synthesis of silver and silver sulfide nanocrystals *via* selective cleavage of chemical bonds, *Nanotechnology*, 2013, **24**, 355602.
31 S. I. Sadovnikov, A. A. Rempel and A. I. Gusev, Nanostructured silver sulfide: synthesis of various forms and applications, *Russ. Chem. Rev.*, 2018, **87**, 303–327.
32 S. I. Sadovnikov, A. I. Gusev, E. Y. Gerasimov and A. A. Rempel, Facile synthesis of Ag_2S nanoparticles functionalized by carbon-containing citrate shell, *Chem. Phys. Lett.*, 2015, **642**, 17–21.
33 S. I. Sadovnikov, A. I. Gusev, E. Y. Gerasimov and A. A. Rempel, Silver sulfide nanoparticles with a carbon-containing shell, *Inorg. Mater.*, 2016, **52**, 441–446.
34 *X'Pert HighScore Plus software package, Version 2.2e (2.2.5)*, PANalytical B. V. Almedo, The Netherlands, 2009.
35 A. I. Gusev and A. A. Rempel, *Nanocrystalline Materials*, Cambridge Intern. Science Publ., Cambridge, 2004, p. 351.
36 S. I. Sadovnikov, A. I. Gusev and A. A. Rempel, Nonstoichiometry of nanocrystalline monoclinic silver sulfide, *Phys. Chem. Chem. Phys.*, 2015, **17**, 12466–12471.
37 S. I. Sadovnikov, A. I. Gusev and A. A. Rempel, Artificial silver sulfide Ag_2S: crystal structure and particle size in deposited powders, *Superlattices Microstruct.*, 2015, **83**, 35–47.
38 J. Hunter, *Zeta Potential in Colloid Science: Principles and Applications*, Academic Press, London, 1988.
39 Y. V. Kuznetsova, A. A. Kazantseva and A. A. Rempel, Zeta potential, size, and semiconductor properties of zinc sulfide nanoparticles in a stable aqueous colloid solution, *Russ. J. Phys. Chem. A*, 2016, **90**, 864–869.
40 *Gatan Misroscopy Suite*, Version 2.31.734.0, Gatan Inc.
41 http://www.gatan.com.
42 S. I. Sadovnikov and A. I. Gusev, Structure and properties of Ag_2S/Ag semiconductor/metal heteronanostructure, *Biointerface Res. Appl. Chem.*, 2016, **6**, 1797–1804.
43 R. Sadanaga and S. Sueno, X-ray study on the α-β transition of Ag_2S, *Mineral. J.*, 1967, **5**, 124–148.
44 T. Blanton, S. Misture, N. Dontula and S. Zdzieszynski, *In situ* high-temperature X-ray diffraction characterization of silver sulfide Ag_2S, *Powder Diffr.*, 2011, **26**, 110–118.
45 X.-F. Qian, J. Yin, S. Feng, S.-H. Liu and Z.-K. Zhu, Preparation and characterization of poly-vinylpyrrolidone films containing silver sulfide nanoparticles, *J. Mater. Chem.*, 2001, **11**, 2504–2506.
46 X. Lu, L. Li, W. Zhang and C. Wang, Preparation and characterization of Ag_2S nanoparticles embedded in polymer fibre matrices by electrospinning, *Nanotechnology*, 2005, **16**, 2233–2237.
47 G. Hong, J. T. Robinson, Y. Zhang, S. Diao, A. L. Antaris, Q. Wang and H. Dai, *In vivo* fluorescence imaging with Ag_2S quantum dots in the second near-infrared region, *Angew. Chem., Int. Ed.*, 2012, **51**, 9818–9821.
48 D. Ruiz, B. del Rosal, M. Acebrón, C. Palencia, C. Sun, J. Cabanillas-Gonzalez, M. Lopez-Haro, A. B. Hungría, D. Jaque and B. H. Juarez, Ag/Ag_2S nanocrystals for high sensitivity near-infrared luminescence nanothermometry, *Adv. Funct. Mater.*, 2016, **27**, 1604629.
49 M. Cai, C. Ding, X. Cao, F. Wang, C. Zhang and Y. Xian, Label-free fluorometric assay for cytochrome c in apoptotic cells based on near infrared Ag_2S quantum dots, *Anal. Chim. Acta*, 2019, **1056**, 153–160.
50 P. Jiang, C.-N. Zhu, Z.-L. Zhang, Z.-Q. Tian and D.-W. Pang, Water-soluble Ag_2S quantum dots for near-infrared fluorescence imaging *in vivo*, *Biomaterials*, 2012, **33**, 5130–5135.
51 S. Lin, Y. Feng, X. Wen, P. Zhang, S. Woo, S. Shrestha, G. Conibeer and S. Huang, Theoretical and experimental investigation of the electronic structure and quantum confinement of wet-chemistry synthesized Ag_2S nanocrystals, *J. Phys. Chem. C*, 2015, **119**, 867–872.
52 Y. Zhang, Y. Liu, C. Li, X. Chen and Q. Wang, Controlled synthesis of Ag_2S quantum dots and experimental determination of the exciton Bohr radius, *J. Phys. Chem. C*, 2014, **118**, 4918–4923.
53 M. S. Smirnov and O. V. Ovchinnikov, IR luminescence mechanism in colloidal Ag_2S quantum dots, *J. Lumin.*, 2020, **227**, 117526.
54 L. E. Brus, Electronic wave functions in semiconductor clusters: experiment and theory, *J. Phys. Chem.*, 1986, **90**, 2555–2560.
55 S. H. Ehrlich, Spectroscopic studies of AgBr with quantum-size clusters of iodide, silver, and silver sulfides, *J. Imaging Sci. Technol.*, 1993, **37**, 73–91.
56 P. Lalanne and J. Hugonin, Interaction between optical nano-objects at metallo-dielectric interfaces, *Nat. Phys.*, 2006, **2**, 551–556.